Rheological, Mechanical, Thermal, and Morphological Properties of Polypropylene/Ethylene-Octene Copolymer Blends

ANA LÚCIA N. DA SILVA,[1] MARISA C. G. ROCHA,[2] FERNANDA M. B. COUTINHO,[1,3] ROSÁRIO BRETAS,[4] CARLOS SCURACCHIO[4]

[1] Instituto de Macromoléculas Professora Eloisa Mano/UFRJ, P.O. Box 68525, 21945-970, Rio de Janeiro, RJ, Brazil

[2] Instituto Politécnico/UERJ, Nova Friburgo, RJ, Brazil

[3] Departamento de Processos Industriais, IQ/UERJ, Rio de Janeiro, RJ, Brazil

[4] Departamento de Engenharia de Materiais/UFSCar, São Carlos, SP, Brazil

Received 7 December 1998; accepted 19 May 1999

ABSTRACT: Rheological and morphological studies were performed on polymer blends of ethylene-octene copolymer [polyethylene elastomer (PEE)] and polypropylene (PP). The viscosities of PEE, PP, and PEE/PP blends were analyzed using an Instron capillary rheometer and a Rheometrics Dynamic Stress Rheometer, SR 200. A non-Newtonian flow behavior was observed in all samples in the shear rate range from 27 to 2700 s^{-1}, whereas at shear rates in the range from 0.01 to 0.04 s^{-1}, a Newtonian flow behavior was verified. The scanning electron micrographs showed that dual-phase continuity may occur between 50 and 60 (wt %) of PEE. This result is consistent with the Sperling's model. The mechanical analysis showed that PEE/PP, with 5 wt % of PEE, presented an increase on the mechanical properties and as the PEE content increased, a negative deviation in relation to an empirical equation was observed. Thermal analysis showed that there were no change in the crystallization behavior of the matrix when different elastomer contents were added. Dynamic mechanical thermal analysis showed that samples with low PEE contents presented only one peak, indicating a certain degree of miscibility between the components of these blends.
 J Appl Polym Sci 75: 692–704, 2000

Key words: polymer blends; polyolefin elastomer; polypropylene, properties

INTRODUCTION

A new family of ethylene/α-olefin copolymers of narrow molecular weight and high degrees of comonomer distribution has been produced by metallocene technology. Because these materials are elastomeric in nature, one of the uses for them is to improve impact properties for brittle polymers such as polypropylene (PP) at low temperatures. According to the manufacturer, polyethylene elastomer (PEE) can compete against ethylene-propylene-diene terpolymers (EPDM) in the production of PP-based blends because of their pellet form, which allows for faster mixing and broader handling and compounding options.[1–8]

Many articles have reported on the influence of the blending process on the relationships between

Correspondence to: F. M. B. Coutinho.
Contract grant sponsors: PRONEX, CAPES, CNPq, PADCT/CNPq, and PADCT/FINEP.

Journal of Applied Polymer Science, Vol. 75, 692–704 (2000)
 CCC 0021-8995/00/050692-13

morphology and final properties of rubber/i-PP blend systems.[9–12] Therefore, in the present work, a systematic study has been performed to investigate PP-based blends containing commercial ethylene/1-octene copolymer (PEE) as a second component. The main goal of this work was to investigate how the molecular structure and PEE content may determine the melt rheology behavior of blends and correlate it with the morphology, thermal and mechanical properties of those systems.

EXPERIMENTAL

Material and Blend Preparation

Isotactic PP (KM 6100) was donated by Polibrasil Resinas (Rio de Janeiro, RJ, Brazil), and PEE (EG 8100, with 24 wt % of comonomer), produced by Dow Chemical Company (Freeport, TX), was donated by Branco.

A Wortex single screw extruder, model H210, was used for melt blending the PEE/PP systems, containing different weight percents of PEE: 0% (sample A′), 5% (sample A), 20% (sample B), 40% (sample C), 50% (sample D), 60% (sample E), 80% (sample F), and 100% (sample G). The screw speed was set at 80 rpm and the temperature profile in the extruder from the feed to the metering zone was set at 220°C.

Rheological Measurements

A flow curve has two distinct regions—the Newtonian region and the power law region. The Newtonian region is observed at very low shear rates, where the viscosity is constant. This viscosity is called the zero shear viscosity. At high shear rates, the power law region, the viscosity η decreases with increasing shear rates. In this region, η can be expressed as

$$\eta = m\gamma^{n-1} \quad (1)$$

where n is the power law index and m is the consistency.

The steady state flow properties of PEE, PP, and PEE/PP blends were measured in an Instron capillary rheometer (model 4204) using a 0.7645-mm diameter capillary with a length of 76.0 mm. Measurements were made at 220°C over a shear rate range from 27 to 2700 s^{-1}. The true shear stress ($\tau\omega$), true shear rate ($\gamma\omega$), and melt viscosity (η) were calculated using standard procedures.

The oscillatory flow properties, namely the complex viscosity η^* (defined as $\eta^* = \eta' - i\eta''$, where η' is the dynamic viscosity or the real part of the viscosity and $i\eta''$ is the imaginary part of the viscosity), the storage modulus, G' (defined as $G' = \omega\eta''$, where ω is the frequency of the oscillations in rad/s) and the loss modulus, G'' (defined as $G'' = \omega\eta'$) of the pure polymers and blends, were determined at 220°C in a Rheometrics Dynamic Stress rheometer—SR 200, in the cone-plate mode at an angular frequency range from 0.01 to 100 rad/s.

Morphology Examination

The morphology of the blends was examined in a Jeol scanning electron microscope (SEM), Model JSM-5300. Samples were cryogenically fractured in liquid nitrogen and etched with heptane to extract the elastomer phase during 7 days and then dried for ≈5 h at 80°C, followed by gold coating before their examination.

Mechanical Behavior

The tensile tests were conducted at room temperature (25°C and 55% relative humidity) using samples obtained by compression molding on an Instron Tester (model 4204), according to ASTM D882, at a strain rate of 50 cm · min^{-1}.

Thermal Analysis

A Perkin Elmer DSC-7 apparatus was used to determine the melting and recrystallization behavior of the pure polymers and PP blends. Differential scanning calorimetry (DSC) tests were run at a heating rate of 10°C · min^{-1} and a cooling rate of 10°C · min^{-1}.

The measurements of the linear dynamic mechanical properties were made using a dynamic mechanical thermal analyser—DMTA MK III (Rheometric Scientific Ltd., software release 5.41) using sample specimens with the following dimensions: length 24 mm, width 9 mm, and thickness ≈ 2.0 mm. The loss tangent (tan δ) was measured between −60 and 200°C at a constant frequency of 1 Hz and a heating rate of 1°C · min^{-1}.

RESULTS AND DISCUSSION

Capillary Rheometer Results

Values of the exponent n or the flow behavior index of the power law equation

Table I Flow Behavior Index of PEE, PP, and Blends at 220°C

Sample Designation	Power Law Exponent, n
A′	0.35
A	0.35
B	0.37
C	0.35
D	0.37
E	0.40
F	0.47
G	0.60

$$\tau_\omega = m\dot{\gamma}_\omega^n \quad (2)$$

were calculated from the relation of shear stress and shear rate by linear regression. It can be observed that n values are in the range 0.35–0.60 (Table I). A high value of the PEE flow behavior index (n = 0.60) was obtained because the capillary rheological analysis of this material had to be conducted in a low shear rate range because of a limitation of the experiment. The effect of the blend composition on the value of n was not significant. Similar results were also reported for the EPDM/PP and EPDM/high density polyethylene (HDPE)/PP systems.[13] Figure 1 shows that the viscosities of the pure polymers and PEE/PP blends decreased as the shear rate increased, indicating pseudoplastic behavior of the melts at 220°C. It also can be seen that a more significant increase in blend viscosities is obtained from sample E at high shear rates.

It has been reported[14,15] that the viscosity of a polymer blend can be described by using the log additivity principle:

$$\ln \eta_b = \sum w_i \ln \eta_i \quad (3)$$

where w_i, η_i are the weight fraction and the viscosity of each blend component, respectively, and η_b is the viscosity of the blend.

Theoretical values of viscosity at a constant shear rate were evaluated for the PEE/PP blends and they are listed in Table II. It can be observed that, for samples A and B, the theoretical and experimental viscosity values are close for all shear rates analyzed. This behavior suggests that, at lower PEE content, an interdiffusion of the polymer chains across the phase boundaries should occur readily, resulting in enhancement of the component interaction. As the PEE content increases, a negative deviation in relation to the additivity principle is observed. This behavior has been attributed to a tendency to phase separation in the blends.[16]

Rheometrics Dynamic Stress Rheometer Results

Figure 2 shows the dependence of the logarithm of the value of the complex viscosity (η^*) on the logarithm of investigated frequencies for PEE, PP, and PEE/PP blends. As shown, for the whole range of explored frequency, PEE/PP blends exhibit a decrease in viscosity value with increasing frequency, i.e., PEE/PP blends are pseudoplastic melts. It is also observed that PEE presents a lower viscosity at lower frequencies and as the PEE content increases, the viscosity of the systems decreases. This behavior can be related to the fact that the addition of 5 (wt %) of PEE tends to increase the average end-to-end distance between PP coils, and thus interactions between PP molecules may occur. As the PEE content increases, the distance between PP coils tends to increase, reducing the occurrence of interactions between PP molecules and consequently the viscosity of the blends decreases. For higher frequencies, the PEE/PP blend viscosities are between the viscosities of the pure components (PEE and PP), and these values increase as the PEE content increases (Fig. 2). This result can be attributed to the fact that at higher frequencies the effect of the presence of PEE long chain branches is more significant and entanglements between branching and the chain segment of PEE and PP may occur. As a consequence, an increase in viscosity values is observed as the PEE content increases. The rheological behavior of PEE can be compared with the flow properties of linear low density polyethylene (LLDPE) resin. It has been reported that, at very high rates, as would be encountered in pro-

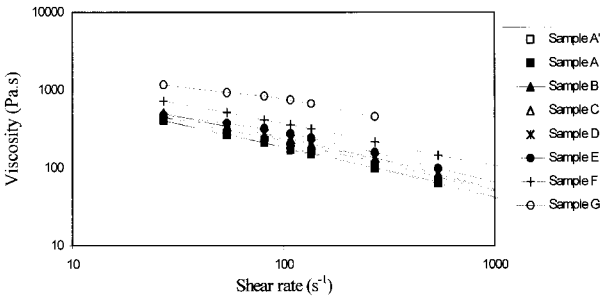

Figure 1 Shear rate versus shear viscosity for the pure components and blends.

Table II Melt Viscosity of PP, PEE, and PEE/PP Blends at 220°C (Length/Diameter = 100)

Sample Designation	Shear Rate $\dot{\gamma}$ (s^{-1})	Shear Viscosity η (Pa · s)	Theoretical Viscosity $\ln \eta_b = \Sigma w_i \ln \eta_i$
A′	55	277	
	110	177	
	270	101	
A	55	265	294
	110	170	190
	270	98	109
B	55	309	353
	110	214	236
	270	122	136
C	55	341	450
	110	227	314
	270	131	185
D	55	350	509
	110	233	363
	270	135	215
E	55	376	574
	110	275	419
	270	158	250
F	55	519	732
	110	360	558
	270	216	337
G	55	934	
	110	744	
	270	456	

cessing, the LLDPE viscosity decreases at a slower rate, indicating that this material also presents a less severe shear thinning than PEE in the same conditions.[17]

It was reported in the literature[18] that the Cross model can be used to model the shear rate dependence of the viscosity of ethylene/octene copolymers produced by metallocene technology (eq. 3):

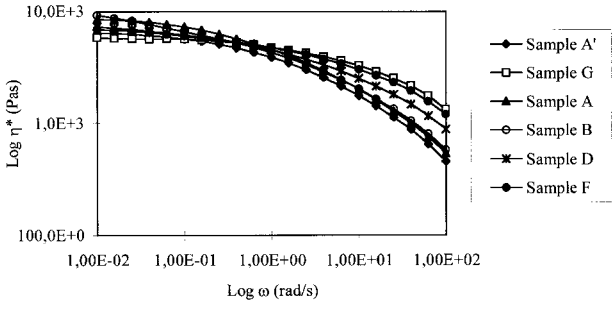

Figure 2 Log (η^*) versus log (ω) for PEE, PP, and PEE/PP blends.

$$\eta = \frac{\eta_0}{[1 + (\eta_0 \dot{\gamma}/\tau^*)]^{(1-n)}} \tag{4}$$

in which τ^* is a constant determined from the intersection of the Newtonian viscosity asymptote and the power law region asymptote. In eq. (3), highly shear thinning fluids have shorter values of n. The parameter η_0/τ^* in eq. (3) is also referred to as the relaxation time τ_0. This equation has the following limiting behaviors:

$$\eta \approx \begin{cases} \eta_0(T, P) \Rightarrow \dot{\gamma} \rightarrow 0 \\ m(T, P)\dot{\gamma}^{n-1} \Rightarrow \dot{\gamma} \rightarrow 0 \end{cases}$$

where

$$m(T, P) = (\tau^*)^{1-n} \cdot \eta_0^n(T, P)$$

and T and P are the temperature and pressure of the process, respectively.

It can be noted that at $\gamma = \tau^*/\eta_0$, eq (3) reduces to

Table III Values of Zero Shear Viscosity (η_0) and Characteristic Relaxation Time (τ_0) for PEE, PP, and PEE/PP Blends

Sample	η_0 (Pa · s)	τ_0 (s)	n
A′	5830	0.344	0.35
A	7778	0.477	0.35
B	7755	0.546	0.37
D	7209	0.369	0.37
F	6234	0.116	0.47
G	5553	0.072	0.60

$$\eta/\eta_0 = \left(\frac{1}{2}\right)^{1-n}$$

such that the shear-stress level is

$$\tau = \eta\dot{\gamma} = \left(\frac{1}{2}\right)^{(1-n)} \eta_0 \cdot \frac{\tau^*}{\eta_0}$$

That is,

$$\frac{\eta}{\eta_0} = \left(\frac{1}{2}\right)^{(1-n)} \text{ at } \frac{\tau}{\tau^*} = \left(\frac{1}{2}\right)^{(1-n)}$$

According to Iwakura et al.,[19] the η_0/τ^* ratio (τ_0) is related to the size of the apparent flow unit; the reciprocal of τ_0 corresponds to the shear rate at which $\eta/\eta_0 = \frac{1}{2}$. The η_0, n, and the characteristic relaxation time (τ_0) values of single components and PEE/PP blends are listed in Table III.

Zero shear viscosity of pure polymers and blends were obtained from Rheometrics Dynamic Stress rheometer data at 220°C as shown in Figure 3. It is clear from this plot that the pure polymers (PP and PEE) present very close η_0 values. It is also observed that the addition of 5 wt % of elastomer (sample A) caused an increase on the η_0 of the PEE/PP blend. However, higher increases of PEE content promoted a decrease on the η_0 of the blends in relation to the sample A. These results can also be explained by the fact that at lower PEE content, the tendency for PP entanglements to occur increases and the consequence is an increase in the blend viscosity.

According to Martuscelli et al.,[20] lower τ_0 means that non-Newtonian flow starts at a larger shear rate, i.e., the material exhibits a larger Newtonian flow range. As can be seen, PEE (sample G) presents the lowest τ_0 value, indicating that this polymer presents the largest range of Newtonian behavior. The higher n value suggests that for such material there is less severe shear thinning in the non-Newtonian region. Sample F also shows a low τ_0 value and a high n value, suggesting that this blend presents similar flow behavior in relation to sample G. When 5 and 20 wt % of PEE is added (samples A and B), the τ_0 values increase and the n values decrease, suggesting that for these blends the non-Newtonian flow starts at lower shear rate and as a consequence they show high shear thinning. These results are in agreement with the flow behavior shown in Figure 2.

As indicated in the literature,[21,22] all viscoelastic materials behave more or less solid-like (elastic) and liquid-like (viscous) depending on the rate at which they are being deformed. This behavior is related to the fact that strained macromolecules tend to pull back to the original shape. The dynamic storage modulus, G', is related to the elastic behavior of the material and may be considered as the amount of the stored energy. The dynamic loss modulus, G'', represents the amount of dissipated energy. The dependence of G' and G'' on the frequency measures the relative motion of all molecules in the bulk and can give important information about the flow behavior of melts.

In Figure 4 the dependence of the elastic modulus G' on the investigated frequencies of PEE/PP blends is compared with those of the pure polymers. An expanded scale of the elastic behavior of the pure polymers and blends at lower frequencies is also included.

As shown, at low frequencies, G' values of samples A and B are higher than those of the pure blend components. Samples D and F (with the highest PEE contents) present G' values between those of the pure polymers. Assuming that G' is related to the stored energy, the above finding indicates that samples with lower PEE contents

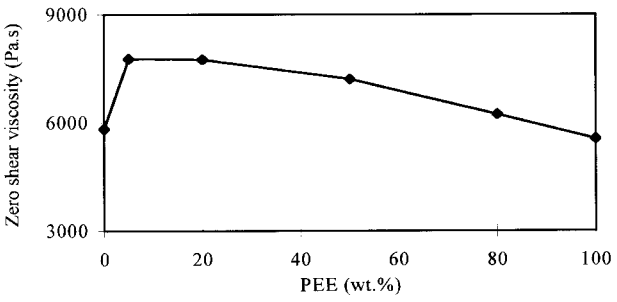

Figure 3 Zero shear viscosity versus PEE content.

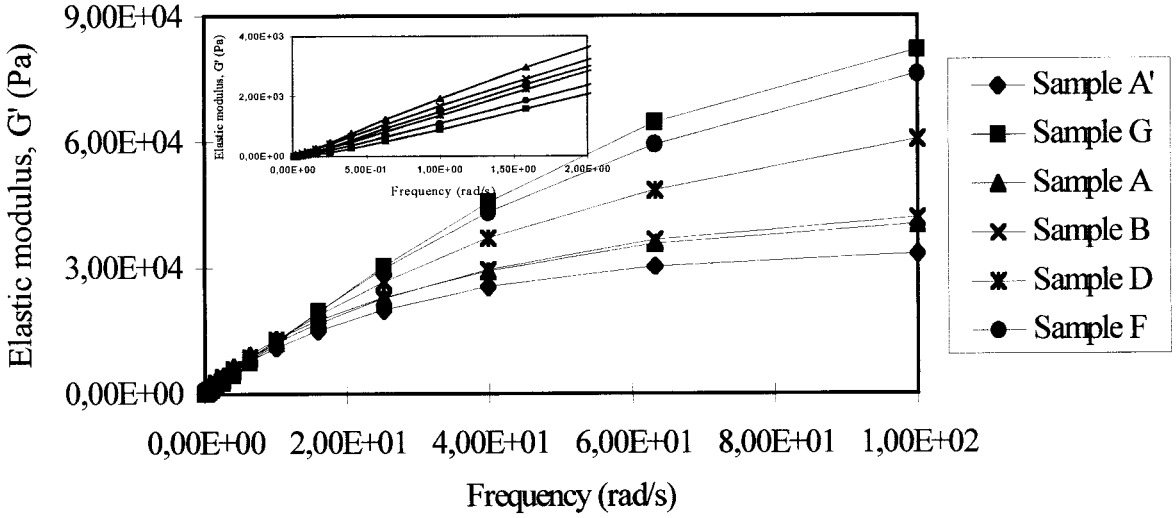

Figure 4 Elastic modulus, G', versus frequency for PEE, PP, and PEE/PP blends.

have higher elasticity at low frequencies. This behavior can also be attributed to the formation of PP entanglements. It can also be observed that PEE presents lower G' values, indicating that this material has lower elasticity at low frequencies. This behavior probably is a result of a conformation change of the molecule due to the occurrence of main-chain entanglements ("coils"). At higher frequencies, G' values of the blends are between those of the pure polymers. The elasticity of the blends increases with the PEE content as a result of the presence of the entanglements between branching and chain segment of PEE and PP. At high frequencies, PEE present higher G' values, indicating that the long chain branches present in PEE molecules tend to produce entanglements and thus a higher elasticity can be observed.

The dependence of the loss modulus, G'', on the investigated frequencies of PEE/PP blends and of the pure polymers is shown in Figure 5. As can be seen, for all examined blends, G'' values are between those of pure polymers at the frequency range analyzed. Taking into account that the dynamic loss modulus G'' represents the amount of dissipated energy, such findings indicate that, with the addition of PEE, materials with higher dissipated energy are produced. At low frequencies, only sample A presents different behavior—this sample has higher G'' values in relation to

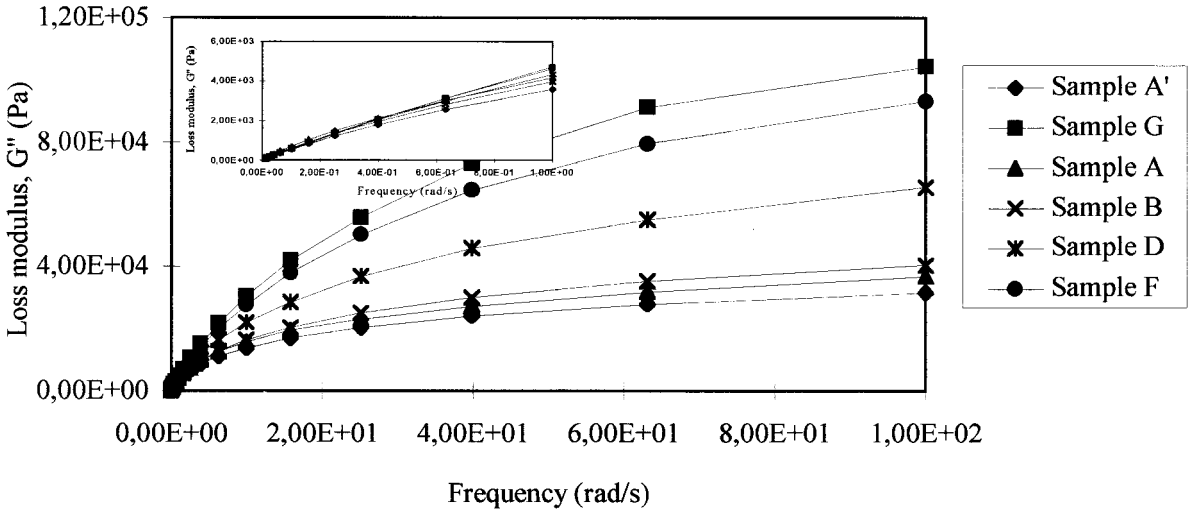

Figure 5 Loss modulus, G'', versus frequency of PEE, PP, and PEE/PP blends.

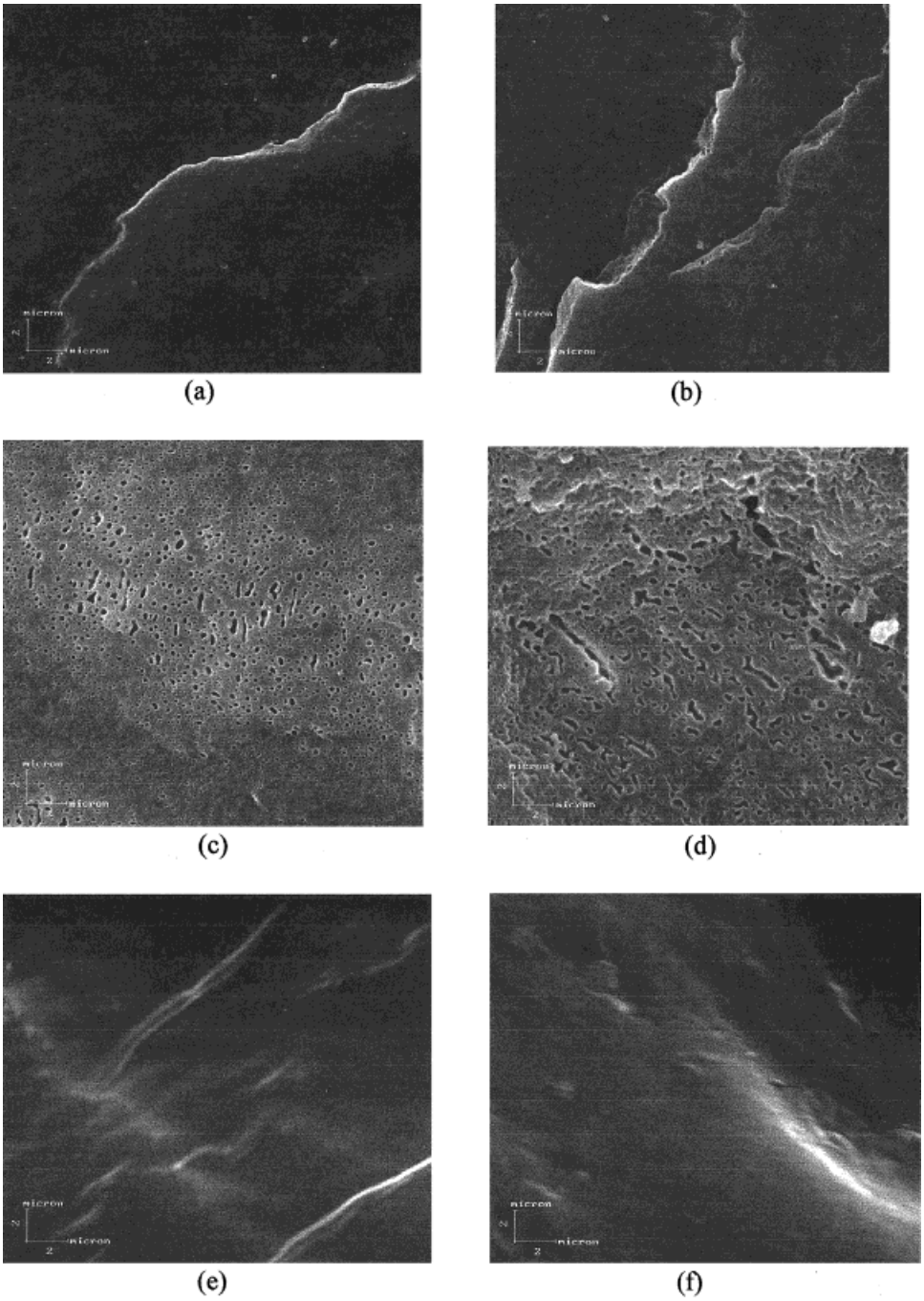

Figure 6 SEM micrographs of samples (a) A, (b) B, (c) C, (d) D, (e) E, and (f) F (see Table IV).

sample B, indicating that the dissipated energy by sample A is higher than that dissipated by sample B in the low frequency range.

SEMs

It has been reported that the rheological properties of elastomer/plastic blends can be related to the mode and state of dispersion of the minor component.[23] Martuscelli and coworkers[20] showed that, for EPR/PP systems, η_0 (blend) and τ_0 (blend) values decrease with increasing dispersion coarseness of the minor component.

The analysis of the PEE state of dispersion, carried out by SEM, shows that the minor component segregates in spherically shaped domains

(Fig. 6) and the size of the elastomer domains increases as the PEE content increases. From sample E, a completely different morphology is observed, i.e., one no longer observes domains of the elastomer phase. As can be seen in Table III, the η_0 values decrease with increasing PEE content and τ_0 values increase up to sample B and then tend to decrease. This behavior indicates that a change in morphology probably occurs in the range of composition between 20 and 50 wt % of PEE.

Dual-phase continuity can be investigated by SEMs and is defined as a region of space where each phase maintains some degree of continuity. In general, the estimated elastomer content at the maximum deviation from linear additivity in the characteristic torque-composition graphs lies approximately in the composition range of dual-phase continuity.

$$\tau = \Phi_P \tau_P + \Phi_R \tau_R \tag{5}$$

where τ and Φ represent characteristic torque (at the given screw speed) and volume fraction, respectively, and subscripts P and R denote plastic and rubber components, respectively.

Another way to predict midpoint compositions of dual-phase continuity is by Sperling's model, which may be expressed mathematically as

$$\tau_P/\tau_R \times \Phi_R/\Phi_P \cong 1 \tag{6}$$

If the quantity on the left side of the equation is greater than unity, the elastomer is likely to be continuous; if the quantity is smaller than unity, the plastic is likely to be continuous.

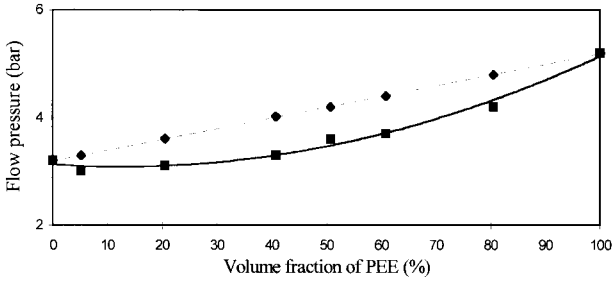

Figure 7 Variation of characteristic flow pressure with composition for PEE/PP blends. The dashed line represents the rule of linear additivity. Squares represent stable flow pressure values, and the solid line is the corresponding second order polynomial fit.

Table IV Volume Fraction and Volume Fraction Ratios of PEE/PP Blends (Where P_P = 3.2 Bar and P_R = 5.2 Bar)

Sample	Φ_P (Vol %)	Φ_R (Vol %)	Φ_R/Φ_P	$P_P/P_R \times \Phi_R/\Phi_P$
A	94.5	5.2	0.05	0.04
B	79.5	20.5	0.26	0.16
C	59.2	40.8	0.69	0.42
D	49.2	50.8	1.03	0.63
E	39.2	60.8	1.55	0.96
F	19.5	80.5	4.13	2.56

In this study, the relationship between torque data and volume fraction was examined by using the flow pressure values, that also characterize the viscous nature. These values were obtained during the blend extrusion. The pure polymers were also processed at the same conditions as the blends. Thus, the following relationship was proposed:

$$P_P/P_R \times \Phi_R/\Phi_P \cong 1 \tag{7}$$

where P is the flow pressure during the processing. Figure 7 shows that the maximum deviation is ca. 44 volume percent (43 wt %) for PEE/PP systems.

Table IV provides the volume fraction and volume ratios for PEE/PP blends. The results show that, according to Sperling's model, for sample E (with 60 wt % of PEE) dual-phase continuity may occur.

Figure 6 shows electron micrographs of etched fracture surfaces of PEE/PP blends. It shows that a gradual-phase inversion has occurred with a region of dual-phase continuity probably in samples with a content of PEE between 50 and 60 wt % (samples D and F). Thus, the SEM results are more consistent with the Sperling's model.

Tensile Strength

Three elements dictate the mechanical properties of polymer blends: crystallinity, morphology, and the interfacial properties. The first one can be estimated from the DSC experiments, the second one from detailed morphological studies, and the last one may be deduced from the mathematical models.

The effect of blend composition on the tensile properties of PEE/PP systems is shown in Table V. It can be seen that as PEE content increases,

Table V Mechanical Properties of PEE, PP, and PEE/PP Blends

Sample	Yield Stress (MPa)	Stress at Break (MPa)	Young's Modulus (MPa)
A′	24.0 ± 1.0	21.0 ± 3.0	390 ± 26
A	25.0 ± 1.0	32.0 ± 5.0	411 ± 16
B	22.0 ± 1.0	27.0 ± 5.0	382 ± 25
C	14.0 ± 0.5	23.0 ± 3.0	237 ± 26
D	6.6 ± 0.2	17.0 ± 1.0	117 ± 9
E	7.0 ± 1.0	17.0 ± 3.0	127 ± 22
F	—	13.0 ± 1.0	37 ± 6
G	—	7.0 ± 1.0	6 ± 1

the Young's modulus decreases as a result of the lowering on the crystallinity of the blends as PEE is added. The stress at break and the stress at yield point also decrease as the PEE content increases. It has been reported in the literature[24] that this behavior is related to the immiscibility of the components and consequent formation of a biphase structure. It is known that the yield and fracture processes on the interphase are accelerated by the immiscibility of the components. It can also be observed that sample A has increased mechanical properties values.

Flaris et al.[25] reported that heterogeneous materials can be described adequately as consisting of a homogeneous and isotropic matrix, in which particles of a second homogeneous phase are dispersed; and, assuming that the volume concentration of the particles is uniform, it should be possible in principle to calculate the properties of its constituents. The experimental values for the Young's modulus are compared to the values obtained by an empirical equation:

Table VI Theoretical and Experimental Values of Young's Modulus of PEE/PP Blends

Sample	Young's Modulus (MPa)	Theoretical Young's Modulus $E_b = E_1\Phi_1 + E_2\Phi_2$
A′	390	—
A	411	370
B	382	311
C	237	233
D	117	195
E	127	157
F	37	81
G	6	—

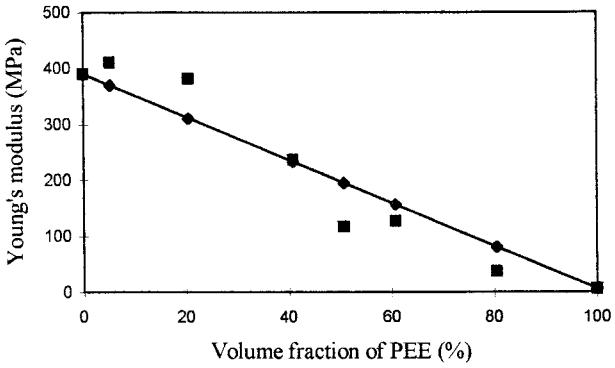

Figure 8 Young's modulus values with composition for PEE/PP blends. The solid line represents the values obtained by eq. (7), and squares represent the experimental values.

$$E_b = E_1\Phi_1 + E_2\Phi_2 \tag{8}$$

where E_1 and E_2 are the Young's moduli of PP and PEE, respectively, and Φ_1 and Φ_2 are the volume fractions of PP and PEE, respectively. The results are listed in Table VI. Figure 8 shows plots of eq. (7) and the experimental Young's modulus data. The results indicate that samples A and B present a positive deviation, indicating that superior interface properties occur between PP and PEE phases. In sample C, the experimental values are close in relation to the theoretical data. As the PEE content increases, a negative deviation is observed, indicating that a poor adhesion between the two components may occur. These results corroborate the rheological results obtained previously.

Thermal Analysis

DSC cooling and heating curves illustrating melting and recrystallization behavior of the pure

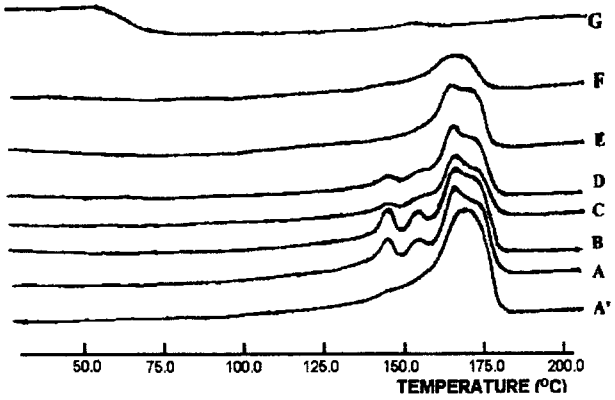

Figure 9 Melting behavior of PEE, PP, and PEE/PP blends.

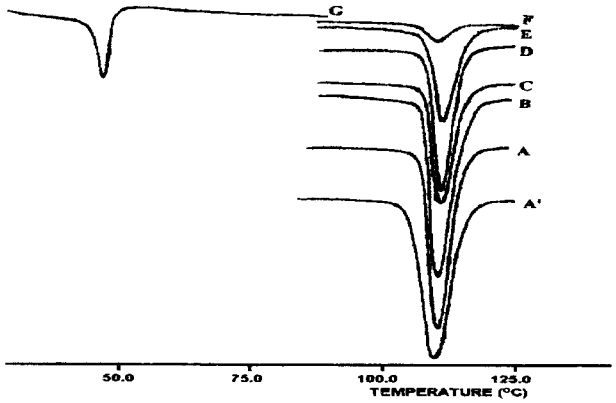

Figure 10 Recrystallization behavior of PEE, PP, and PEE/PP blends.

polymers and PP blends are shown in Figures 9 and 10, respectively. Thermal properties of PEE, PP, and PEE/PP blends are summarized in Table VII. It can be seen that there is practically no change in the crystallization behavior of the PP matrix when different elastomer contents are added ($T_c \cong 110$°C). The PEE curve shows a peak that appears at about 40°C, indicating the presence of a crystalline region.

The melting temperature (T_m) and heat of fusion (H_f) were determined from the heating cycle of a DSC scan. The percentage crystallinity was also calculated by using the relationship

$$\% \text{ crystallinity}(\chi_c) = \frac{\Delta H_f^{\text{obs}}}{\Delta H_f^0} \times 100 \qquad (9)$$

A value of $\Delta H_f^0 = 209$ *J*/g for 100% crystalline PP homopolymer was used for calculating the percentage of crystallinity.[6]

The blends show a broad melting endotherm, which is probably related to changes in the distribution of PP crystal morphology when elastomers are added. The melt temperatures of pure PP and PEE/PP blends occur at ≈162°C, suggesting that the thickness of lamellae is independent of blending of different PEE contents. A melting peak was detected in the PEE melting curve at ≈60°C, indicating a certain degree of crystallinity. As should be expected, the results show that as the PEE content increases, the crystallinity degrees and the heat of fusion decreases in relation to pure PP. Melting thermograms of samples A and B exhibit three distinct melting peaks, indicating an increase in heterogeneity of the crystal size. This melting behavior probably is attributed to the occurrence of miscibility between the blend components.

The temperature dependencies of tan δ of PEE, PP, and PEE/PP blends are shown in Figure 11. It can be seen that sample A′ shows two apparent dispersion peaks at temperatures ≈ 10°C and between 40 and 50°C. These dispersions can be assigned as β and α relaxations, respectively. Numerous studies on the dynamic mechanical dispersions of i-PP have been reported.[26] According to their results, the α-relaxation can be ascribed to intracrystalline chain motion; the β-relaxation corresponds to T_g in amorphous regions. Sample G presents a more accentuated dispersion peak between −50 and −40°C. This dispersion is attributed to micro-Brownian motion of amorphous chains, i. e., glass-rubber transition temperature (T_g). Figure 11 also shows that samples C, D, E, and F present two peaks of tan δ at temperatures between −50 and −40°C and ≈10°C, which are assigned to β_1 and β_2. The higher relaxation peak β_2 is attributed to the T_g of the amorphous region of the i-PP, and the lower relaxation peak β_1 is identified as the T_g of the PEE. For samples A and B only the β_2 peak is observed, indicating a certain degree of miscibility between the components of these blends. These results are in accordance with the results of the rheological analysis.

CONCLUSIONS

A study concerning the influence of molecular structure and PEE content on the melt rheology behavior, on the morphology, and on the mechanical and thermal properties of PEE/PP blends is reported. The following results should to be noted:

Table VII Physical Properties of PEE, PP, and PEE/PP Blends

Sample	T_c (°C)	T_m (°C)	ΔH_f (J/g)	Crystallinity (%)
A′	110	163	93	44
A	111	164	71	34
B	111	162	53	25
C	112	162	36	17
D	111	162	36	17
E	110	162	22	11
F	110	161	13	6
G	42	60	—	—

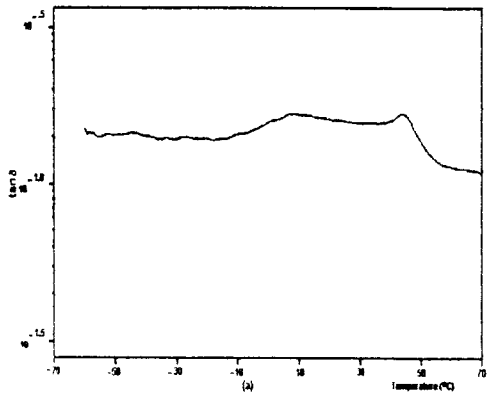
tan δ
Temperature (°C)
(a)

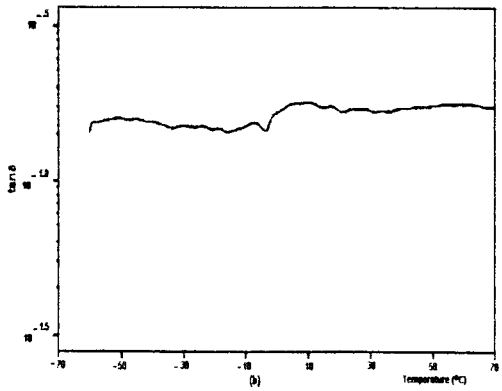
tan δ
Temperature (°C)
(b)

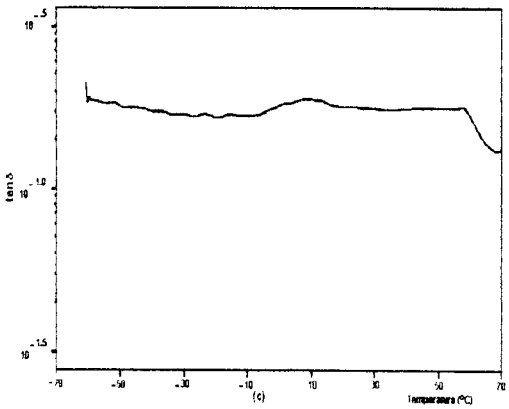
tan δ
Temperature (°C)
(c)

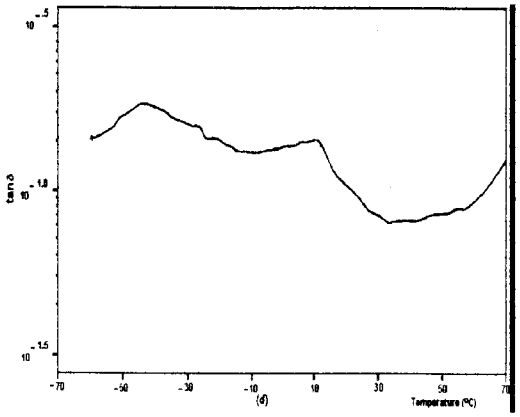
tan δ
Temperature (°C)
(d)

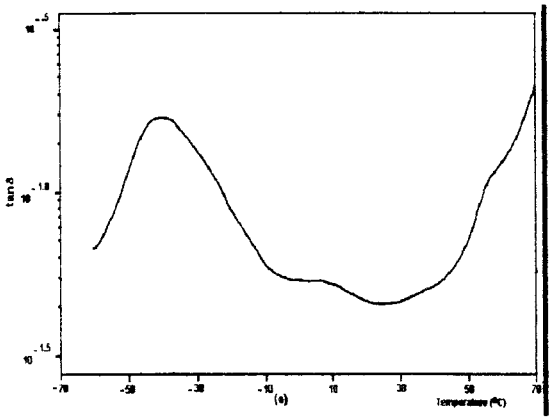
tan δ
Temperature (°C)
(e)

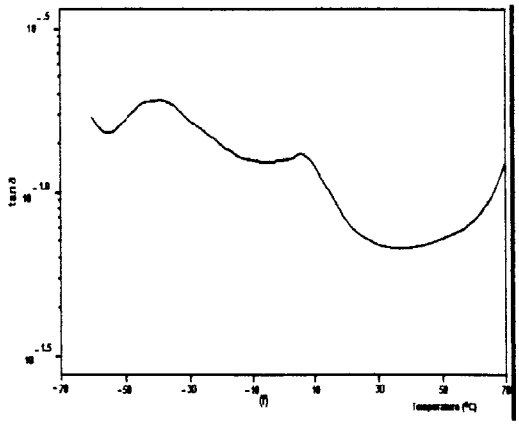
tan δ
Temperature (°C)
(f)

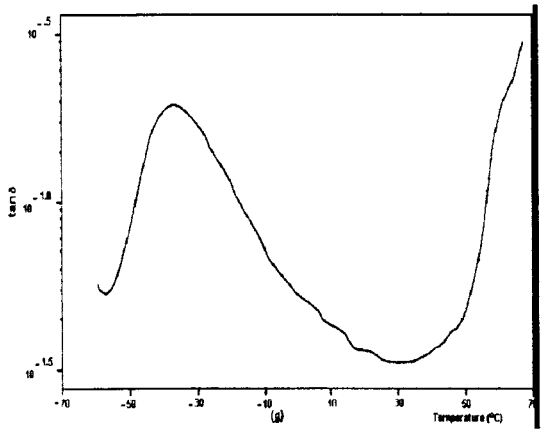
tan δ
Temperature (°C)
(g)

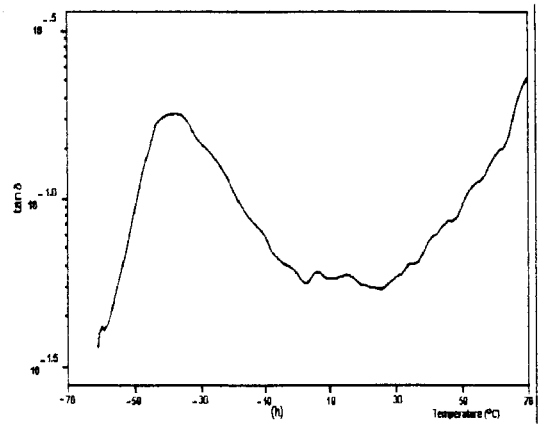
tan δ
Temperature (°C)
(h)

1. The viscosities of PEE, PP, and PEE/PP blends decrease as the shear rate increases, indicating pseudoplastic behavior of the melts at 220°C.
2. The theoretical and experimental values of samples A and B are close in all shear rates analyzed, indicating that at lower PEE content, an interdiffusion of the polymer chains through the phase boundaries should occur, resulting in enhancement of the component interaction. As the PEE content increases, a negative deviation in relation to the additivity principle is observed, indicating a tendency for a phase separation in the blends.
3. At lower frequencies, PEE presents the lowest viscosity and as the PEE content decreases, the viscosity of the systems increases. This behavior can be attributed to the average end-to-end distance between PP molecules that tends to increase as the PEE content increases.
4. At higher frequencies, the values of PEE/PP blend viscosities are between the values of the pure component viscosities, and these values increase as the PEE content increases. This behavior can be related to the effect of the presence of PEE long chain branches that becomes more significant and thus entanglements between branching and chain segments of PEE and PP can occur.
5. At lower frequencies, G' values of samples A and B are higher than those of the pure polymers, indicating that samples with lower PEE contents have higher elasticity.
6. At higher frequencies, the elasticity of the blends increases with the PEE content. This behavior is a result of the presence of the entanglements between branching and chain segment of PEE and PP.
7. The Cross model is applied to describe the rheology of PEE, PP, and PEE/PP blends.
8. The morphology studies showed that dual-phase continuity may occur in blends between 50 and 60 (wt %) of PEE. This result is consistent with the Sperling's model.
9. The mechanical studies showed that sample A has enhanced mechanical properties.
10. The experimental values for the Young's modulus are compared with the values obtained by an empirical equation. It is observed that samples A and B present a positive deviation, indicating that superior interface properties occur between PP and PEE phases. As the PEE content increases, a negative deviation is observed, indicating that poor adhesion between PEE and PP may occur.
11. Thermal analysis shows that there is no change in the crystallization behavior of the matrix when different elastomer contents are added. It is also verified that as the PEE content increases, the crystallinity degree and the heat of fusion decrease in relation to PP. Samples A and B exhibit three distinct melting peaks, indicating the occurrence of miscibility between the blend component.
12. Dynamic mechanical thermal analysis shows that samples A and B present only one peak corresponding to the T_g of i-PP, indicating a certain degree of miscibility between the components of these blends.

Financial support by PRONEX, CAPES, CNPq, PADCT/CNPq, and PADCT/FINEP is gratefully acknowledged. We are also grateful to POLIBRASIL RESINAS, NITRIFLEX, BRANCO, CENPES/PETROBRÁS, and QUIMBARRA (White Martins).

REFERENCES

1. Bailey, M. S.; Brauer, D. Mod Plast 1993, 11, 12.
2. Gupta, A. K.; Ratnam, B. K.; Srinivasan, K. R. J Appl Polym Sci 1992, 45, 1303.
3. Randall, J. C. Exxon Chem. Pat. EP O 351 208, 1990.
4. Silva, A. L. N.; Coutinho, F. M. B.; Rocha, M. C. G. Plást Mod 1996, 40, 264.
5. Borruso, A. V. TECNON Petrochemical Seminar, Rio de Janeiro, Brazil, November 1994.
6. Silva, A. L. N.; Coutinho, F. M. B.; Rocha, M. C. G.; Tavares, M. I. B. J Appl Polym Sci 1997, 66, 2005.
7. Kale, L. T.; Plumley, T. A.; Patel, R. M.; Jain, P. Antec 1995, 2249.
8. Lai, S.; Plumley, T. A. Antec 1994, 1814.
9. Buckmall, C. Toughened Plastic; Applied Science: London, 1977.

Figure 11 Tan δ values of PEE, PP, and PEE/PP blends: (a) sample A′; (b) sample A; (c) sample B; (d) sample C; (e) sample D; (f) sample E; (g) sample F; and (h) sample G (see Table VII).

10. Kinoch, A. J.; Young, R. J. Fracture Behavior of Polymer; Applied Science: London, 1989.
11. Ishikawa, M. Polymer 1995, 36, 2203.
12. Ishikawa, M; Sugimoto, M.; Inoune, T. J Appl Polym Sci 1996, 62, 1495.
13. Choudhary, V.; Varma, H. S.; Varma, I. K. Polym J 1991, 32, 2541.
14. Ferry, J. D. Viscoelastic Properties of Polymers; John Wiley & Sons: New York, 1970.
15. Rohn, C. L. Analytical Polymer Rheology: Structure-Processing-Properties Relationships; Hanser Publishers: New York, 1995.
16. Schreiber, H. P.; Olguin, A. Polym Eng Sci 1983, 3, 129.
17. Doak, K. W. In Encyclopedia of Polymer Science and Engineering; Mark, H. M.; Bikales, N. M.; Overberg, C. G.; Menges, G., Eds.; John Wiley & Sons: New York, 1970; Vol. 6.
18. Plumley, T. A.; Lai, S. Y.; Betso, S. R.; Knight, G. W. Antec 1994, 1221.
19. Iwakura, K.; Fujimura, T. J Polym Sci 1975, 19, 1427.
20. D'Orazio, L.; Mancarella, C.; Martuscelli, E. Polymer 1991, 32, 1186.
21. Dealy, J. M.; Wissbrun, K. F. Melt Rheology and Its Role in Plastic Processing; Van Nostrand Reinhold: New York, 1990.
22. Lenk, R. S. Polymer Rheology; Applied Science Publishers: London, 1978.
23. Thamm, R. C. Rubber Chem Technol 1976, 50, 24.
24. Lovinger, A. J.; Williams, M. L. J Appl Polym Sci 1980, 25, 1703.
25. Flaris, V.; Stachurski, Z. H. J Appl Polym Sci 1992, 45, 1789.
26. Yamaguchi, M.; Miyata, H.; Nitta, K. J Appl Polym Sci 1996, 62, 87.